Distribution Agreement

In presenting this thesis as a partial fulfillment of the requirements for a degree from Emory University, I hereby grant to Emory University and its agents the non-exclusive license to archive, make accessible, and display my thesis in whole or in part in all forms of media, now or hereafter know, including display on the World Wide Web. I understand that I may select some access restrictions as part of the online submission of this thesis. I retain all ownership rights to the copyright of the thesis. I also retain the right to use in future works (such as articles or books) all or part of this thesis.

James Sebel December 2, 2011

Measuring Interfacial Viscosity Using Macro- and Micro-rheology

by

James Sebel

Dr. Eric R. Weeks
Adviser

Department of Physics

Dr. Eric R. Weeks

Adviser

Dr. Connie Roth

Committee Member

Dr. Jed Brody

Committee Member

Dr. James Flannery

Committee Member

December 2, 2011

Measuring Interfacial Viscosity Using Macro- and Micro-rheology

By

James Sebel

Dr. Eric R. Weeks

Adviser

An abstract of
a thesis submitted to the Faculty of Emory College of Arts and Sciences
of Emory University in partial fulfillment
of the requirements of the degree of
Bachelor of Arts with Honors

Department of Physics

2011

Abstract

Measuring Interfacial Viscosity Using Macro- and Micro-rheology
By James Sebel

We measure the viscous moduli of thin films using two different methods. First, we use a magnetic needle viscometer. Our apparatus employs Helmholtz coils to control the position and orientation of the needle in the film. By driving the needle we can produce a response in the film which allows us to probe the bulk viscous properties of thes film. Second, we use single particle microrheology to probe the local properties of the film. Tracking the mean-squared displacement of particles as they undergo Brownian motion probes the local viscous properties of the surface. Coupling this technique with the magnetic needle viscometer provides information on the effect local viscous properties have on the bulk properties.

We begin with a general introduction to surface rheology and the techniques involved. Then we discuss the experimental techniques, including the method of building the magnetic needle viscometer, why certain decisions regarding its construction were made, the micro-rheology technique and sample preparation. The results section includes unexpected deviations in our experiments and possible reasons for these. Finally, the discussion highlights the future directions of the project.

Measuring Interfacial Viscosity Using Macro- and Micro-rheology

By

James Sebel

Dr. Eric R. Weeks

Adviser

A thesis submitted to the Faculty of Emory College of Arts and Sciences
of Emory University in partial fulfillment
of the requirements of the degree of
Bachelor of Arts with Honors

Department of Physics

2011

Acknowledgements

A special thank you to Dr. Eric Weeks for all his help and guidance through this project and over the years preceding it. Thank you to everyone in the lab, both past and present, for all your assistance with IDL, troubleshooting all aspects of the experiment, and keeping the lab fun. And finally, thank you to my committee members; for some of you I know this outside of your usual field of expertise.

Table of Contents

Introduction

Surfactants play an important role in many aspects of our daily lives; from food sciences, to shaving creams, to biological processes within our own bodies, surfactants are there. Imagine the head of foam on your favorite beer. The size of the bubbles, the length of time they persist and the texture of them is due in large part to the properties of the surfactant in the beer. Surfactants also play a crucial role in breathing; indeed some premature babies are unable to breathe unassisted due to problems related to surfactant production in the lungs [1, 2].

So what is this mysterious substance that helps us breathe and shave uninhibited? Surfactant is short for "surface-active agent," and it is composed of a hydrophobic tail and a hydrophilic head. These molecules, which run the gamut from proteins to soap, like to sit at the boundaries of water. Whether it is water and air or water and oil, they align themselves with their heads in the water and their tails out of the water as in Figure 1. The particular surfactant we used for our experiments is called Human Serum Albumin, (HSA) which is an abundant protein in human blood.

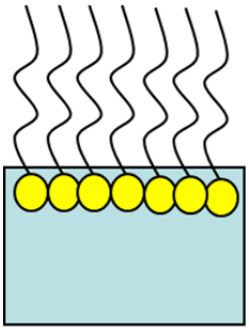

Figure 1. The hydrophobic tails of surfactants stick out of the water and into the air while the hydrophilic heads remain in the water.

There are several ways to measure bulk viscosity. Some methods are simple, like watching a weighted ball sink in a tube where the force due to gravity (after accounting for any buoyant effects) is balanced by the viscosity of the fluid, while some are more complicated, like using a rotating plate to shear the liquid inducing a flow field. In the

rotating plate viscometer, the known torque and angular velocity are balanced by the viscosity of the fluid.

Measuring the viscosity of surfaces tends to be somewhat more difficult, and there are still many avenues to be explored. The basic premise remains the same, though: the two methods we used involve putting a probe particle at the surface, inducing some controllable or measurable motion in it, and measuring the effect the surface has on the expected motion. The difference in our two methods comes from the type of probe used. The first method, a magnetic needle viscometer, uses a small, macroscopic, magnetic needle placed at the surface and driven by an external magnetic field which can be controlled. The motion of the needle is then driven by the force of the magnetic field changing and retarded by the viscoelastic properties of the substance. The second method, one particle microrheology, uses a microscopic sphere with a radius of ~1μm. The sphere undergoes motion due to thermal effects. The Brownian motion is related to the viscosity of the surface using the modified Stokes-Einstein equation [3, 4, 5, 6].

There are advantages and disadvantages for both methods. The driven, macroscopic needle is able to probe higher viscosities than the thermally driven probe, but the macroscopic needle is less well able to probe low viscosities. Thermally driven probes are able to probe low viscosities, but are generally unable to probe viscosities above a certain threshold, ~10^{-6} N s / m [7, 8, 9]. So a combination of both methods will allow a larger range of surface viscosities to be probed.

There is a difference in the units of three dimensional or bulk viscosity, Pa*s, and two dimensional or surface viscosity, Pa*s*m, which occurs because of the loss of a dimension in the 2D case. This length term, L, provides interesting information about the

sensitivity of any probe particles used to measure the surface viscosity. $L = \eta_{2d} / \eta_{3d}$ where η_{2d} and η_{3d} are the surface viscosity and bulk viscosity respectively. As η_{2d} the sensitivity of a probe to the surface viscosity also increases. A probe particle with a size about the size of L will probe both the surface viscosity and bulk viscosities equally, but as the size of the probe particle grows larger, the effects of surface viscosity on its motion decrease. Conversely, if the size of the probe particle decreases, the effects of surface viscosity on its motion increase. Thus, from this length scale, the probe particles can be optimized to measure surface viscosity.

Materials and methods

Helmholtz Coils:

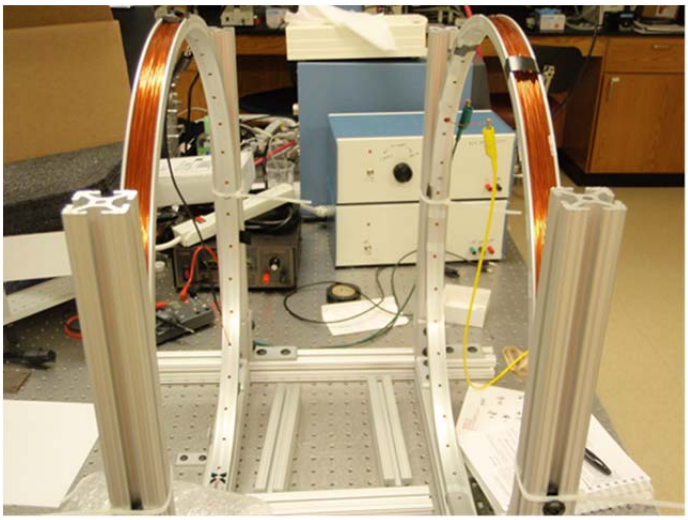

Figure 2. A picture of our Helmholtz coils. The two orange wrapped rings are the coils, and the sample was mounted in the middle on top of a microscope.

We need to be able to induce some force on our magnetic needle. We do this by creating a controlled, uniform, magnetic field at our sample. Our system for controlling the magnetic field involved two electromagnetic coils arranged in such a way that they created a uniform magnetic field between them. This special arrangement of

electromagnetic coils is called a Helmholtz Coil. We followed the procedure by Ding, et al. [10].

The Helmholtz coils Ding used were arranged to produce a uniform magnetic field gradient rather than a uniform magnetic field. For a uniform magnetic field gradient, the separation distance needs to be two times the coil radius. To create a uniform magnetic field the distance between the coils needs to be one coil radius.

We want a uniform magnetic field because ultimately our needle should remain stationary at the center of our sample, and the motion we induce will be rotational motion caused by a 180° change in the direction of the field. This induced torque is the same as a bringing a bar magnet close to a compass. The compass aligns its poles so that the north pole of the compass points to the south pole of the bar magnet. If you then turn the bar magnet around, the compass will also spin through 180° so that the south pole of the compass now points to the north pole of the bar magnet.

According to the Biot-Savart law, the magnetic field, B, of a circular current carrying loop is [11]

$$B = \frac{\mu_0 I R^2}{2(R^2 + x^2)^{3/2}}$$

where μ_0 is the permeability constant, I is the current passed through the coil, R is the radius of the coil, and x is the distance from the coil. For two equivalent electromagnetic coils set one radius apart with the same current running through them so that the magnetic field is in the same direction, the magnetic field at the center is given by

$$B = \frac{\mu_0 N I R^2}{(R^2 + (\frac{R}{2})^2)^{3/2}}$$

where *N* is the number of turns of wire in the coils. A slight modification to that equation yields the magnetic field at any point between the two coils. Figure 3 shows the calculated magnetic field as a function of the percentage of the distance between the coils. This shows the excellent theoretical uniformity in field strength at the center of the coils.

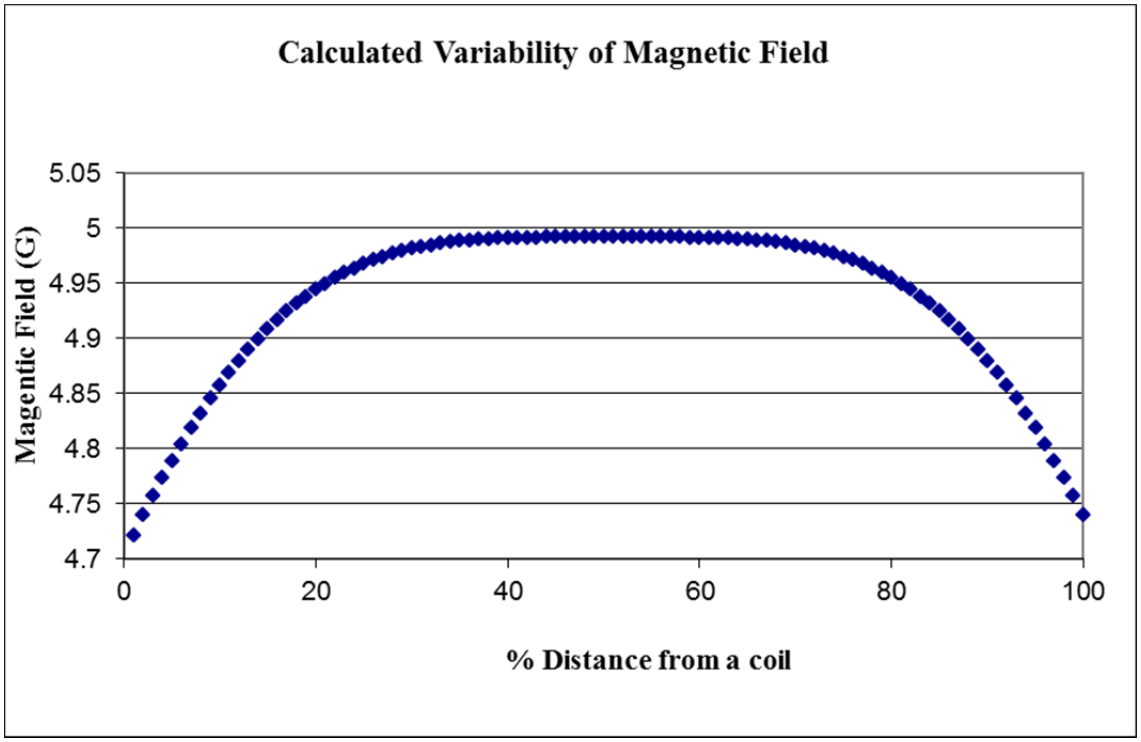

Figure 3. The calculated magnetic field as a function of the percent distance from either coil. The coils and current in the coils are symmetric, hence the symmetry of the plot.

Our coils were made using copper magnet wire hand wound around two aluminum bicycle wheels of radius 0.273 meters. There were 106 winds per coil. The coils were connected in series to insure constant current across them both. Our maximum allowed current, due to limitations from the power supply, was 3.13 amps. However due to other considerations discussed later, experiments were generally conducted at lower currents. We included a double pole double throw switch from Mcmaster-Carr in our

circuit so that the direction the current was flowing could be quickly and easily reversed. The rise time for the circuit was on the order of 1-10 μs. Jon Carr built a trigger device to trigger the high speed camera when the current reversed directions. This was connected in parallel with the coils and triggered when the voltage difference between the nodes changed from positive to negative. We did not connect it in series because we wanted to be able to vary the current without necessarily triggering the camera.

We measured the magnetic field of our coils using a Hall Probe and Gauss Meter (Lakeshore) and found that we had similar uniformity; however, the magnitude of the magnetic field was slightly decreased from the theoretical. This explains the slightly lower deviation in Figure 4 from the expected magnetic field. This could be due to a number of factors.

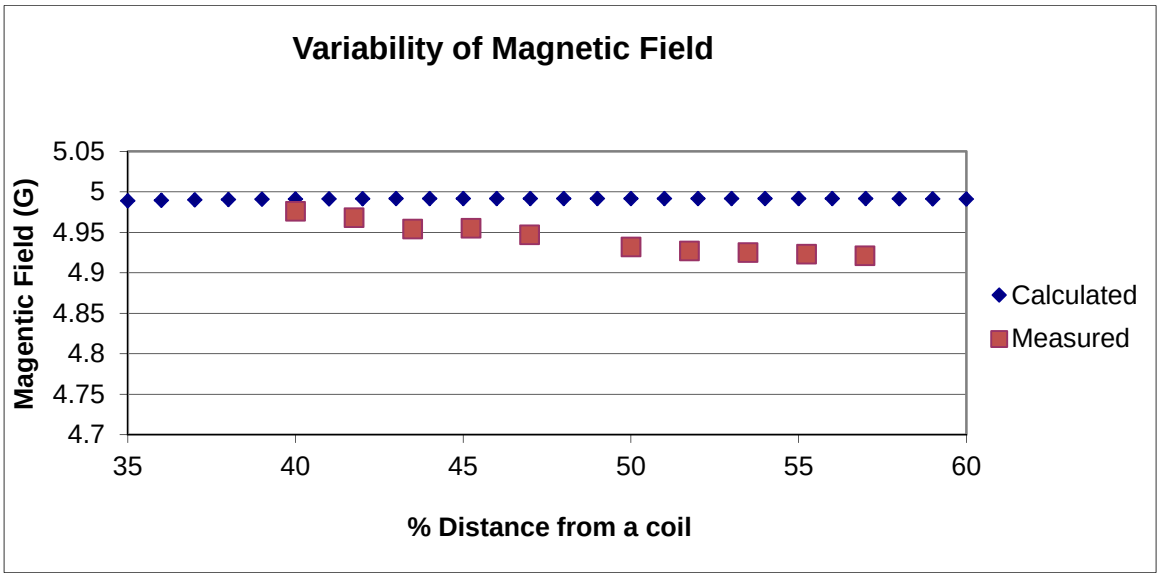

Figure 4. The measured magnetic field and the calculated magnetic field in Gauss plotted versus the percent distance from a coil. The slight deviation of measured magnetic field from calculated magnetic field is most likely due to a rise in temperature of the coils over time which increases their resistance and decreases the current flowing through.

First, there is an ambient magnetic field due to the earth's magnetic field and the electronics in the lab. This ambient field is between 0.3 and 0.5 Gauss. The coils could be aligned in the direction of the ambient field or perpendicular to it which would allow us to produce very small fields; the ambient field on the axis of the Helmholtz coils would simply add, or subtract its contribution depending on the direction of the field produced by the coils.

Second, as the coils have current running through them, they heat up slightly. With higher current they heat up more, and as the temperature increases, the resistance of the coils increases. Therefore, assuming our power supply outputs constant voltage, the current in the coils decreases; as seen in Chart 1. This effect can be minimized and practically eliminated by using lower voltages, or by allowing the coils to rest and cool down between experiments. The decrease in current is subtle but noticeable at the maximum voltage provided by our power supply, but as we decrease the voltage, the drop in current disappears entirely. The experiments are usually conducted at 1.5 amps, and since we have a variable voltage power supply, the voltage output was changed to maintain a constant current. The third cause could be due to imprecision in the winding of the coils, as these were wound by hand and are not ideal Helmholtz coils. However, each coil taken by itself performed close to the theoretical expectations of a current carrying loop.

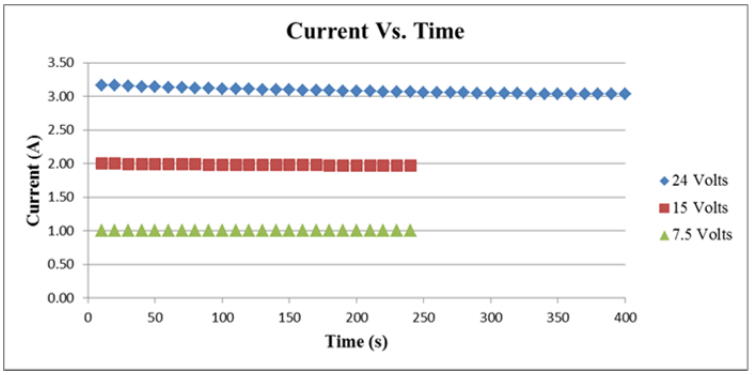

Chart 1. Current as it changes with time in the coils for three different voltages. Experiments are usually conducted at 1.5 Amps, and the variable voltage is changed to maintain the current.

Magnetic Needle:

Our apparatus has at its heart a rotating needle. All the other aspects are ways of manipulating and measuring the needle's rotation, but ultimately our probe is the needle. This means that we need to optimize our needle for the experiment, recognizing that the effects of our sample on surface viscosity will be affected by our needle's size.

Since we are probing surfaces, our probe particle, whether a needle or microscopic sphere, will be affected by the bulk liquid, in our case water, the monolayer we are trying to probe, and the air above the surface. The probe will stick out of the monolayer into the air and into the water below; therefore any viscosity we measure will be some combination of all three viscosities. Since air is orders of magnitude less viscous than the substances we are looking at, we ignore its contribution. Nevertheless, we cannot ignore the effects on the viscosity due to the bulk water below our monolayer. Thus, the thinner the profile of our probe, the more we will probe the monolayer itself.

Initially we followed the needle design by Ding et al. [10] which was a 1.5 mm diameter by 8 mm long magnetic stir bar centered in the middle of 3 cm of hollow Teflon tubing. The tubing was necessary to keep the stir bar, which was made of dense, magnetic material, floating at the surface. We then covered the tubing in white Teflon tape to

provide a uniform, bright, white background for imaging the needle, as can be seen in figure 5 (a). There were distinct disadvantages with this needle.

Figure 5. A) Our old needle made from a magnetic stir bar in plastic tubing. It is covered in Teflon tape to increase the surface tension between it and water. The size difference and curvature of the old needle are clearly visible. It is 3.65 mm thick. B) Our new needle made of rolled steel. We covered it the top surface in white tape to make imaging it easier. It is .2 mm thick.

First, the tube was slightly curved, which resulted in a non-uniform probe depth. Since the ends curled up somewhat, the center tended to be immersed deeper than the two ends, which tended to be in the air somewhat.

Second, the tubing tended to get liquid in it, which made it less buoyant. Sealing the ends was possible; however, this then made modifications to the needle more difficult.

Third, and most important, was the diameter of the needle. With this method, the needle's diameter was a little over 3.5 mm. When you consider that the layers we intended to study are on the order of a single molecule thick, a 3.5 mm thick probe seems oversized. A result of this size discrepancy is that we are primarily probing the bulk fluid underneath our monolayer, thus in order to measure any difference, the viscosity of the monolayer would need to be substantially larger than that of the bulk fluid. The Boussinesq number can model the relationship between particle size and measured effect [12, 13, 14].

$$\mathrm{Bo} = \frac{\eta_s}{\eta a}$$

Where η_s is the surface viscosity, η is the bulk viscosity, and a is the characteristic length of your probe. For our needles a is the length. As Bo increases η_s dominates the sample, and as Bo decreases the effects of the bulk viscosity dominate.

Due to the above considerations, we searched for a more effective needle. As previously mentioned, the reason our needle was so large was because of the additional plastic tubing to buoy the needle. Magnets are notoriously dense. They tend to be made of iron or other heavy metals. They are also difficult to mold and shape into odd specifications. Part of this is due to the way they are made. Permanent magnets can be made in several ways, but the end result tends to be brittle. This makes sanding them smaller impossible. Or else they are made of fine, powdered metals compressed and sealed with some protective layer. In order to make a true permanent magnet, the magnet must be heated above its Curie temperature (determined by the properties of the composition of metals) and placed in a strong magnetic field. It then must be allowed to cool slowly while still in the magnetic field. This adds just one more layer of difficulty in producing magnets.

We searched for companies capable of making smaller magnets but were unable to find one that was already able to produce magnets on the scale we needed. Some of the companies were willing and able to build the necessary machinery to make these thinner magnets, but they tended to want a minimum order of 50,000 pieces and even at ten cents per piece, this was extraordinarily expensive and excessive.

In order to get rid of the plastic tubing our magnet would need to stay at the surface of its own accord. That means the surface tension would have to be sufficient to keep the magnet afloat. We calculated that a sufficiently thin needle made of common

magnetizable metals needed to be thinner than about 0.5 mm or approximately 0.02 inches. That ensured the weight of the magnet would be supported fully by the surface tension of water. We actually sought an even thinner magnet, both because the Bo number would be larger, and because as surfactant is added it then decreases the surface tension of the liquid. So to probe higher viscosities and concentrations of surfactant we needed a thinner needle.

Unfortunately, we couldn't find anyone to manufacture a needle that thin, but Dr. Weeks had the brilliant idea of taking some type of metallic foil and magnetizing it ourselves. We found a rolled steel company that specializes in metal foils. They have a type of steel that is easily magnetizable and maintains its magnetic domains in a uniform direction. The company sent us a two-foot sample of one of their foils, which was 0.05 mm thick and 0.5 mm wide. Because it is pressed metal, needles made with this metal are very thin rectangular prisms rather than the cylinder we were previously using. In order to provide consistent imaging we covered one face of the needle with white tape which faced up out of the liquid which is visible in figure 5 (b).

Inducing permanent magnetism proved to be more difficult than we expected. As mentioned above, creating a permanent magnet requires heating above the Curie temperature and cooling in the presence of a strong magnetic field. The Curie temperature for steel tends to be around 700 degrees Celsius; however, since our new needle was made from a proprietary form of steel, the exact Curie temperature is unknown. This temperature is nonetheless attainable, but as the steel is heated it begins to oxidize more readily, leaving the needle with inconsistencies in its profile. Specifically, under these conditions the steel tends to bubble and bulge in odd ways, like blisters. This

would obviously affect our experiment. As we determined, the way to fix this is to immerse the needle in an inert gas atmosphere while heating it, which can be done by flushing argon over it, preventing the oxygen from reaching the heated steel. This method does not allow for direct heat from a flame to be applied to the needle, as fire requires an oxygen rich environment. There are ovens which can reach these temperatures and be filled with an inert gas atmosphere, but placing the necessary equipment to generate the magnetic field inside the oven is impossible.

Because of the difficulties of generating permanent magnetism in the needle we sought other methods of creating a magnet. Steel takes on magnetism when the molecules within its crystalline structure are allowed to move and rearrange in the presence of magnetic field. The magnetic field introduces order into the otherwise disordered arrangement of electrons and the effects become compounded, thereby creating a strong, uniform field. The addition of heat frees the electrons, but the presence of a very strong magnetic field can also induce some order. Placing steel in the presence of a magnetic field without heating it will never produce as strong a magnet; however, it will induce some permanence to the magnetism of the steel.

There are two easy methods for creating a weak permanent magnet. The first method is to stroke the steel you wish to magnetize over the surface of a strong magnet. Neodymium or other rare earth magnets work well. If you stroke the steel in only one direction then the steel's magnetism will be stronger. The issue with this method is that it is difficult to control, and the exact orientation of magnetism can be difficult to ascertain.

The second, preferred method is to place the steel in the center of a solenoid. A large solenoid's magnetic field at its center behaves like an infinitely long solenoid, thus

the magnetic field is uniform. If the steel needle is placed in the center of the solenoid parallel to the solenoid's length, then the needle will be magnetized as a bar magnet with the poles being along the long axis, rather than a plate magnet where the poles would be the two faces of the rectangular needle; see figure 6.

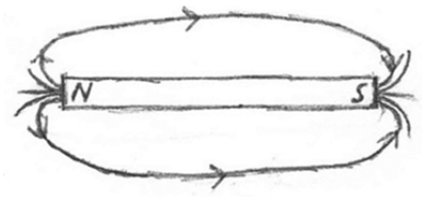

Figure 6. A diagram of the magnetism of the magnetic needle. It is magnetized like a bar magnet.

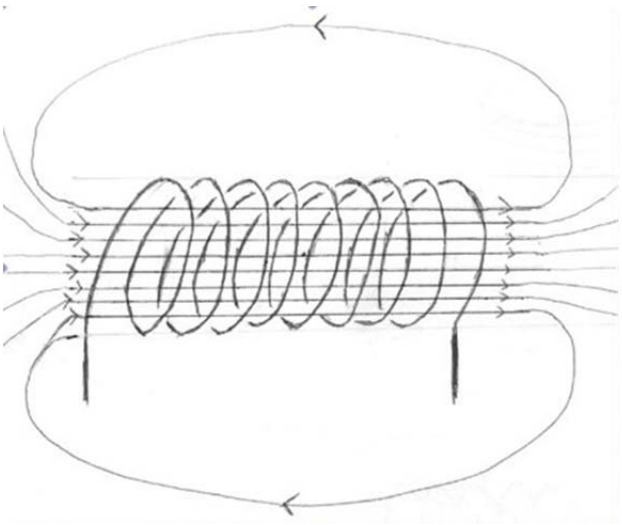

Figure 7. In the center of a solenoid the magnetic field is very strong and uniform in one direction, which is perfect for magnetizing our needle.

We used a solenoid provided by Dr. Bing to magnetize the needle. The magnetic field within an infinite solenoid looks like figure 7 and is given by [11]

$$B = \frac{\mu_0 N I}{L}$$

Where N is the number of turns, μ_o is the magnetic permeability $4 * \pi * 10^{-7}$ N/A^2, I is the current in the circuit, and L is the length of the solenoid. The solenoid was wrapped 1000 times, and current used was 1.2 Amps to generate the magnetic field. The solenoid is 7

cm long, so the estimated magnetic field at its center acting on our 2 cm steel needle is about 215 Gauss. This is many times the magnetic field strength of our Helmholtz coils and we magnetized the needle for 90 seconds. We found that this was a sufficiently long time to create permanence in the needle. Preliminary observation did not exhibit a decrease in the magnetic strength of the needle over time or when placed within the Helmholtz coils Further exploration into this will be necessary to ensure consistency across experiments.

High-Speed Camera:

In order to image the needle rotating we used a Phantom v9 High Speed camera. Selecting an appropriate camera for the project required extensive research that included communicating with several companies about our needs and their capabilities as well as negotiating with them to reach an affordable price. During the process several interesting considerations came up.

First, a product of any high speed camera is that as you increase the number of frames per second (the frame rate) the amount of available light decreases. This becomes clearer when you consider the exposure time for each frame. At thirty frames per second the exposure time is 33 milliseconds, whereas at 1000 frames per second the exposure time is one millisecond. The corresponding decrease in available light is linear with exposure time; however, there are light enhancing devices like those used by the military for night operations. Unfortunately, those enhancing devices are not compatible with high speed cameras because, by their very nature, the enhancing devices require longer exposure times.

A second consideration, and one that had the greatest effect on purchasing considerations (second, of course to price), was that of an onboard hard-drive. At higher frame rates, the camera may be imaging a frame every 33 microseconds (or even more quickly), and at present there is no data transfer system, whether usb 2.0 or Ethernet, which can transfer the information from the camera to a computer that quickly. So an onboard hard-drive stores the images which are then downloaded at leisure. The greatest effect this has on the experiment is time related. Every additional gigabyte of onboard hard-drive space corresponds to additional video length. Storing one megapixel images at 1000 frames per second on a one gigabyte hard-drive roughly corresponds to only one second of imaging.

The final feature inherent in high speed imaging is the physical image size in pixels. Very much related to the above two issues, at higher frame rates the number of pixels per image must decrease. This is partly due to the light limitations and imaging speed issues, but it is more an effect of the hard-drive size. As the frame rate increases to its max (in our case around 150,000 frames per second) at max resolution the camera would require more than 250 gigabytes of hard-drive to take even one second of images!

We ended up purchasing a camera with a 6 gigabyte onboard hard-drive, which can take approximately 1800 maximum resolution frames at 500 frames per second. This translates to 3.5 seconds for our films, which is sufficient time and speed for most of our needle spins, and adjusting these settings to take a longer or shorter film as necessary is simple.

Sample Preparation:

There were several reasons why we chose to use Human Serum Albumin (HSA), the foremost of which was because a previous member of our lab, Vikram Prasad [6], had some success with it. It was helpful to be able to consult with Vikram about any questions and issues. Other reasons are because it is a well-studied molecule in all fields of science, the time it takes HSA to rise to the surface has been well documented [15], and particularly because there are several interfacial rheology papers that use it, including [6, 7].

Unfortunately, as we learned with time and repeated experiments, HSA is a complex molecule which can be difficult to handle. Reproducibility has been an issue with this project, due in large part to the changes that can occur to the viscosity of HSA with subtle changes to its environment. For instance, isopropanol which we is often added to microscopic particles to help spread them at the surface, may functionally change HSA, causing it to form dense micelles which, if they remain at the surface can create pockets of incredibly high viscosity. The micelles formed may also sink, and if enough HSA is affected, then the viscosity at the surface becomes that of water. Other issues we have discovered with time are that the pH of the solution can be critical to the viscosity, that the viscosity is related closely to the temperature of the sample, and that it may take substantial time to dissolve completely in water. As we did not know we would encounter these issues with the sample preparation we continued trying to troubleshoot it. A different sample could have been used, and, if we knew then what we know now, we probably would have performed the calibrations to the magnetic needle experiment using an oil layer of known viscosity.

We made solutions of HSA mixed with distilled water, generally at concentrations of 0.03 mg/ml of water. Changing the concentration is a subject of our study; however, the experiments discussed in this paper are all samples with 0.03 mg/ml concentrations of HSA. The HSA was purchased from Sigma Aldrich and comes in a crystalline form. One issue we may have encountered was incomplete dissolution and suspension of the HSA in the water. Longer stirring times seem to have resolved these issues.

One Particle Mean-Squared Displacement:

In addition to the magnetic needle, we used fluorescent particles suspended at the surface to measure the viscosity; see figure 8. The particles were from Invitrogen and were carboxylate modified FluoSpheres. Initially we used 0.5 micron diameter particles; however, due to an issue where the particles seemed to be sticking together creating binary clusters, we switched to the 2 micron diameter particles which did not exhibit this behavior. It appears that the binary clusters may have been an optical effect due to a misaligned light source rather than a physical feature of the probes. However, that has still not been confirmed.

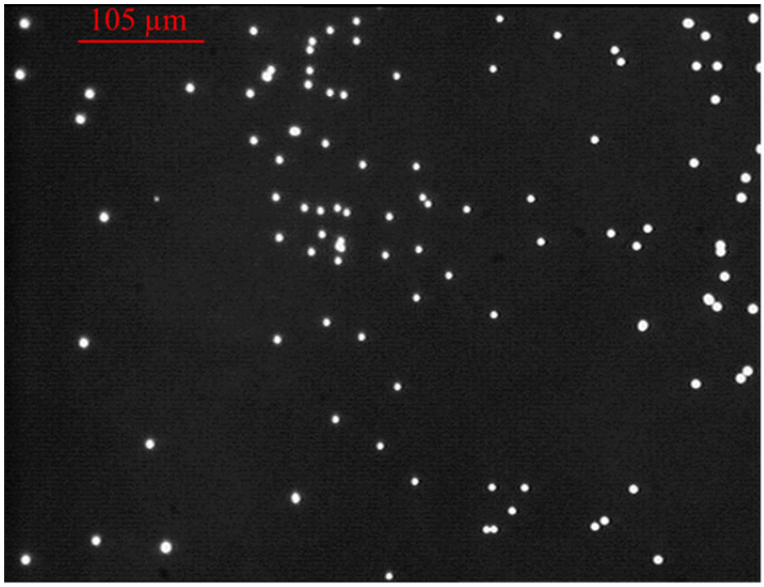

Figure 8. 2 micron diameter probe particles at a surface

To suspend the particles at the surface we added 20% isopropanol to the solution they were in. We then dropped small droplets of isopropanol-water-particle solution on to the surface using a very fine syringe. The alcohol helped both to spread the particles at the surface and keep them fixed at the surface, preventing them from sinking down into the bulk of the sample. One concern with adding alcohol is the potential for adverse interactions between alcohol and HSA, whether by changing the pH of the sample or by functionally changing the molecules. It was observed by eye that pure alcohol mixed with high concentrations of HSA produced a cloudy sample. Hence, to mitigate possible interactions the particles were added to the surface as quickly as possible after pouring the sample. Since HSA requires some time to rise to the surface, we hoped that no functional changes would occur due to the alcohol [15].

Tracking:

We used Interactive Data Language (IDL) produced by ITT Visual Information Solutions to track and analyze the data. For the magnetic needle experiments, Ken

Desmond wrote the code to track the needle's rotation. Figure 9 shows the raw image taken from the camera with the colors inverted to improve contrast, the enhanced image we work with, and the enhanced image with the track line overlaid. We were able to track the needle's rotation very well. For the particle tracking we used a code commonly utilized by our lab for this purpose, as written by John Crocker and David Grier [16].

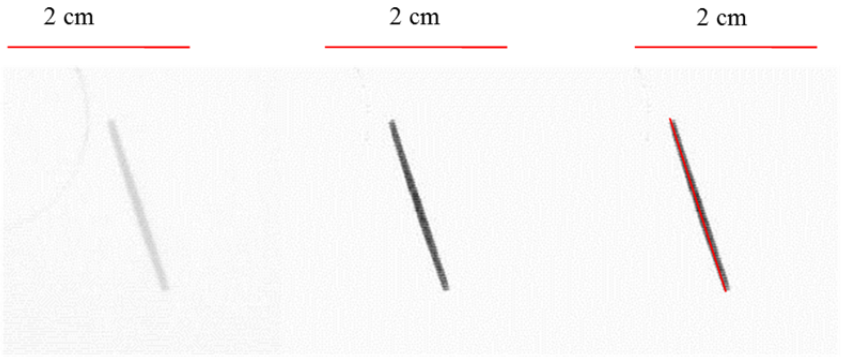

Figure 9. The raw image taken from the camera (left). The enhanced image we work with (center). The enhanced image with the track line overlaid (right). The colors have been inverted to improve contrast.

Results

We were able to track both particles at the surface and a needles rotation for the same concentration of HSA, 0.03 mg/ml. The Mean Squared Displacement (MSD), $\langle \Delta r^2(\tau) \rangle$, of a particle is related to the surface viscosity by a modified Stokes-Einstein relation [3, 4, 5, 6].

$$\langle \Delta r^2(\tau) \rangle = 4D'_s \tau$$

$$D'_s = D_s[\ln\left(\frac{2\eta_s}{\eta a}\right) - \gamma_E + O\left(\frac{\eta a}{\eta_s}\right)]$$

$$D_s = \frac{k_B T}{4\pi\eta_s}$$

Where k_B is Boltzmann's constant, T is the temperature of the sample in Kelvin, η_s is the surface viscosity, η is the bulk viscosity, a is the radius of the particle, γ_E is Euler's constant which equals 0.577, and τ is the lag time in seconds.

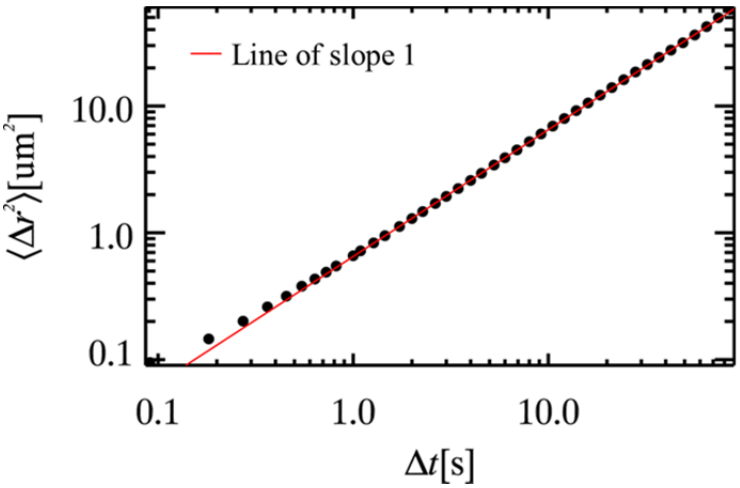

Figure 10. The MSD of a 0.03mg/ml sample of HSA. The line of slope 1 indicates the sample is diffusive in a viscous liquid. $\eta_s = 9.92 * 10^{-8}$ N s / m.

Figure 10 is the plot of the MSD, and from this the surface viscosity calculated for the sample was $9.92 * 10^{-8}$ N s / m, which is very near the surface viscosity measured when there was no surfactant, $5.95 * 10^{-8}$ N s / m. The viscosity measured by Vikram et al. for this concentration of HSA is $34.0 * 10^{-8}$ N s / m [6]. Our measured viscosity is on the same order of magnitude as Vikram's, but given that the viscosity of HSA changes over time, it is possible that this explains why our value is lower [15]. The line of slope one plotted over the points indicates that particles are diffusing with Brownian motion in a purely viscous sample. If the slope is greater than one, this means the particles are more diffusive, or super-diffusive, than should occur from simple Brownian motion. Super-diffusion is commonly caused by drift in the sample. If the slope is less than one, then this indicates a sub-diffusive state. This can be caused by viscoelasticity in the sample.

Similarly, the needle data from the same sample is unaffected by the surfactant. At low Reynolds number, when a magnetic field places a torque on the needle it is balanced by the viscous rotational drag of the sample [14,17]

$$\mu B \sin(\varphi) - \xi_r \frac{d\varphi}{dt} = 0$$

where μ is magnetic dipole moment of the needle, B is the magnitude of the magnetic field, φ is the angle between the wire and the magnetic field, and ξ_r is the rotational drag coefficient. Solving this yields

$$\varphi(t) = 2\tan^{-1}[\exp(-k(t - t_0))]$$

where the angular relaxation rate $k = \mu B / \xi_r$, and t_0 is the time at which φ passes through $\pi/2$., figure 11 is the plot of φ for the 0.03 mg/ml solution of HSA. The red line is a line of best fit from which k can be calculated. k for this sample is 10.9 s^{-1}, which again is similar to water and indicates there may not be effects from the surfactant.

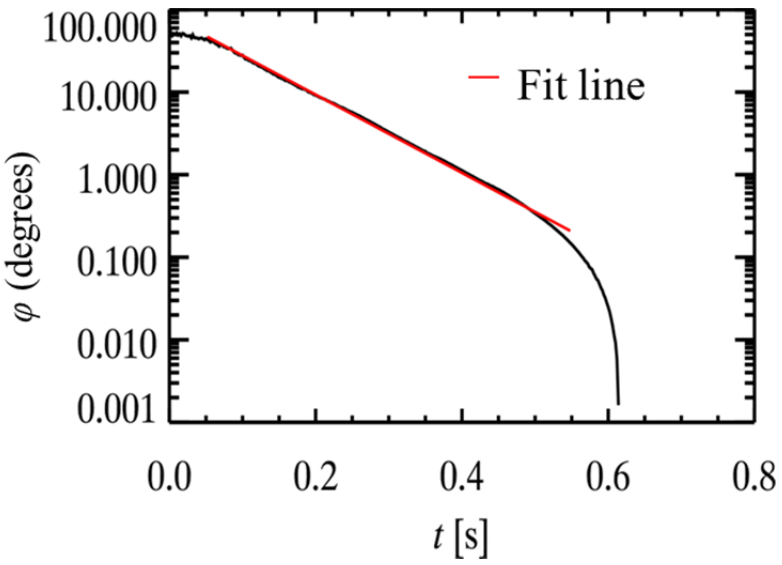

Figure 11. φ plotted as a function of time. A line of best fit is fitted to the data and overlayed. From this, the angular relaxation rate can be calculated.

As with the MSD, a straight line indicates a purely viscous solution. The drop at the end is due to poor resolution in the statistics.

A new member of our lab, Thibaut Divoux, adjusted how the samples were being prepared and, with his help, the samples have become more reproducible as well as more viscous. We did not have ample time to extensively study the samples Thibaut helped prepare for this thesis; however, we were able to look at one sample of 0.03 mg/ml HSA using the needle. Figure 12 is a plot of φ for the sample where the direction of the magnetic field was flipped back and forth several times. The field was turned on in one direction for 15 seconds, and then reversed for 5 seconds. Afterwards, it reversed back to its initial direction for another 5 seconds. This was repeated with 5 second intervals for a minute; however, we have only included the first 30 seconds here.

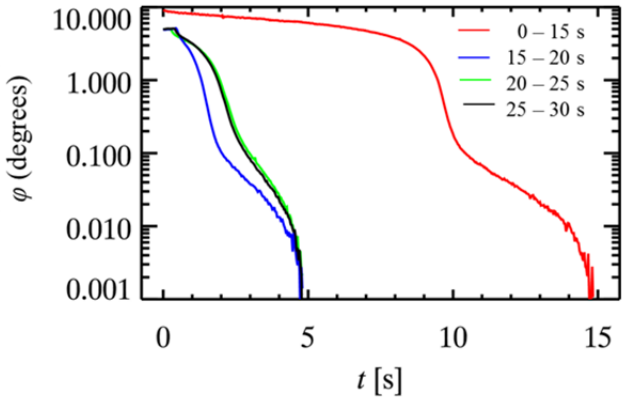

Figure 12. φ for a sample where the direction of the magnetic field was flipped back and forth several times. The field was turned on in one direction for 15 seconds, and then reversed for 5 seconds, and then reversed back to its initial direction for another 5 seconds. This was repeated with 5 second intervals. (The green and black line overlap, making the green line hard to see)

It is clear from this data set that the behavior is not a purely viscous response. Also, the relaxation rate increases after the sample is sheared the first time. This necessitates a standard for conducting these experiments. In order to make the sample "forget" any past history and experiments conducted on it, we rotated the needle 20 times in rapid succession. Our intention was to "clear" the sample, allowing us to produce consistent results. Figure 13 is φ one minute after clearing, 10 minutes after clearing, and 30 minutes after clearing. This shows that waiting only one minute after clearing the sample

may give slightly different results from waiting longer; however, waiting between ten and thirty minutes seems likely to produce consistent results.

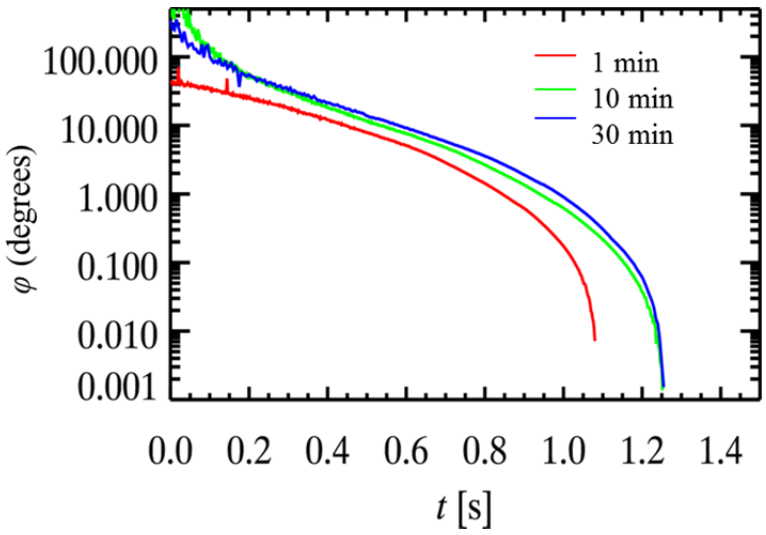

Figure 13. φ 1 minute after clearing the sample, 10 minutes after clearing, and 30 minutes after clearing.

Discussion

Reproducibility in these experiments has always been a challenge. As we are trying to develop and calibrate a different way for our lab to measure viscosity, a consistent sample and procedure would allow future lab members to make sure they are using the device properly and that it is working correctly. Troubleshooting both of these methods is difficult and time consuming, thus streamlining the process is ideal.

With that said, we are hopeful that Thibaut's recent adjustments to the sample preparation process will produce consistent samples. Thibaut noted that a possible reason for inconsistency in the samples was an incomplete mixing and dissolution of the crystals of HSA. This was corrected by stirring the samples gently for more than ten minutes as opposed to the previous method of vortexing the samples vigorously for about half a

minute. The previous method would sometimes produce very viscous samples, or completely dilute samples.

Particle Tracking:

An aspect of the particle tracking which has been problematic before was that in viscous samples (confirmed by the needle), the 2 μm diameter particles appeared to be completely stationary, undergoing no Brownian motion, and locked into the surface. Again, Thibaut noticed that at higher magnifications the beads were indeed vibrating, but not diffusing very far. Using smaller 0.5 μm diameter beads, Thibaut has been able to probe these highly viscous samples. We knew that the larger beads would diffuse more slowly, nonetheless it was thought that with long enough data samples the viscosity could still be probed, although the timescale which is "long enough" may be significantly longer than we were probing.

The diffusion coefficient, D_s, mentioned earlier holds the key to the timescale. As D_s changes according to ~1/r, a change from 0.5 μm diameter to 2.0 μm diameter beads will require 4 times longer videos in order to see the same diffusion. So rather than taking only 200 seconds of video, perhaps for the 2.0 μm diameter beads an 800 second video would be more appropriate.

Needle:

Before the needle apparatus will be useful, a standard protocol needs to be developed. Due to the odd response curves, and their dependence on both the number of times the needle has been rotated and the interval between needle rotations, many

different viscosities could possibly be measured. Perhaps the viscosity 30 minutes after "clearing" is the desired value, for it gives information about the state of the undisturbed surface. On the other hand perhaps the viscosity after 10 rotations in a row is more desired because it is likely this would provide a more consistent value. Ultimately, the procedure will need to be modified for each experiment to ensure that the desired phenomena are probed.

Another aspect of the magnetic needle apparatus that needs to be addressed before it can be applied to different surfaces is the magnetic moment of the needle. The equations and values we are currently able to extract from our data are relations of relaxation time from one sample to another. The angular relaxation rate is related to the viscosity by $k = \mu B / \xi_r$ and, while we know B, the magnetic dipole moment, μ, has not been measured for our needle yet.

The method for measuring the magnetic dipole moment of a magnet is to rotate it in a known field where it is balanced by another known and measurable force, whether inertia, or the earth's magnetic field or some other method. Unfortunately, the small size of our needle makes many of these methods difficult or impossible. One method which may be the most feasible is to perform the above experiments with an oil film of known viscosity. If several such oils are probed over several magnetic fields, the magnetic dipole moment can be calculated [10]. This method is not ideal because there are additional effects that must be considered which may affect the dipole moment calculated. These include additional dipping into the solution caused by the needles motion, changes to the contact angle of the needle (which would affect the Boussinesq number) and other unknown interactions between the oil and needle [14]. These variables be accounted for

and minimized, but measuring the magnetic moment without any additional interactions to consider would be ideal.

The final issue to overcome with respect to the magnetic dipole moment is how well the needle holds its moment over time and in the presence of weak magnetic fields. Since the needle is not a true permanent magnet, its dipole moment may change over time or in the presence of weak magnetic fields like those caused by the earth and electronics. These changes may be small, but in order to get consistent results the dipole moment may have to be measured before every experiment, in which case a simple method for measuring dipole moment is even more crucial. Of course, another solution to this issue would be to create a true permanent magnet with heating and a strong magnetic field as mentioned earlier.

Summary

We built an apparatus for measuring the viscosities of surfaces. Comparing this method to single particle mean squared displacement is the ultimate goal, which would open up a new range of high viscosity surfaces for further exploration. There are still significant calibrations to be made before the apparatus can be used independently of single particle mean squared displacement; however, all of those calibrations are within reach and simply need time. With the working Helmholtz coils, the groundwork has been laid for many, intriguing, future projects.

There are several intriguing avenues for further research, after the needle apparatus has been calibrated sufficiently. First, changing the length of the needle and probing with multiple lengths may reveal information about the yield stress of the

sample. Second, by changing the depth of the bulk solution below the surface we can probe the effect a nearby boundary has on surface viscosity. It is easy to imagine that motion on the surface propagating to the bottom of the sample and back up to the surface may also have further interesting consequences.

Once these techniques have been calibrated, another interesting direction would be to probe a surface using both the needle and the particles at the same time. Probing a controllable, homogeneous layer with both the needle and microspheres could provide valuable information about how the microscopic properties affect the bulk properties of the surface. This experiment could be extended to include heterogeneous layers, which would provide information about the effect of heterogeneous domains on the bulk properties. Currently the two techniques are done separately due to the difficulty of damping out vibrations where the needle apparatus is mounted. Even small vibrations, like electronics on the table, or more radical vibrations through the building, or someone walking near the apparatus can cause the particles to move wildly about the sample. If that can be fixed, then it would be interesting to observe the microsphere's behavior before, during, and after the needle spins.

The logical next steps in this project are to first calibrate the needle apparatus. This should be done using an oil layer of known thickness and viscosity. By performing the experiments outlined above with the oil layer instead of HSA, the magnetic dipole moment can be easily extracted, and effects we had anticipated, but cannot confirm, such as increased dipping as the needle rotates, should become clearer. Confirming the magnetic dipole moment independently of the apparatus is also necessary. These

calibrations will provide a strong grounding for the possible and exciting future experiments

Who is We?

This may be somewhat irregular, but I was asked to include a discussion of who the "we" involved in this thesis is. I use "we" to mean a lot of different people at a lot of different times, and sometimes the "we" is the royal we. Ken Desmond was my mentor and most closely supervised and assisted me with this project. He trained me in the techniques, and then helped me develop the project primarily with suggestions and guidance to keep me on track and grounded. Ultimately, I researched all the components of the magnetic needle apparatus, including the frame and its design, size specifications of the wire, and the high speed camera and its triggering apparatus. I built, tested and troubleshot, the apparatus entirely on my own, with the exception of physically winding the coils, as that was a two person job, where again, Ken helped me. I researched and developed the new, thinner needle and performed all the necessary calibrations magnetizing treatments on it.

On the software side, Ken helped me an enormous amount. I knew nothing about the programming language used in the lab, nor did I know how to track anything. Here again, Ken trained me and mentored me so that I could perform the data analysis on my own, but I made no significant improvements to the programming.

In terms of the sample preparation and troubleshooting HSA, this was very much a group effort. I worked with two other undergraduates in the lab who were also experimenting with HSA to develop a consistent sample and any headway made there

was due in part to each of us. Thibaut Divoux, a post doc who recently joined the lab, has taken on the task of solving the HSA problems, and has made enormous headway; however, his contributions and success could not be applied to this thesis due to time constraints.

Of course, there are a hundred tiny questions I have asked all the members of the lab at one time or another, and bouncing ideas off people removed from the specifics of my project was incredibly helpful. And finally, the orchestrator of all these components and ultimate decision maker was Dr. Weeks. He was not a physical presence in the lab, it is rare to see him working at a microscope these days, but every step of the process required his approval and he had eyes on the ultimate goals of the project. From weekly updates to regular group meetings, Dr. Weeks provided an endless supply of good ideas to keep move the project moving forward.

Citations

[1] M. E. Avery, J. Mead, "Surface properties in relation to atelectasis and hyaline membrane disease," AMA J. Dis. Child., **97**, 517 (1959)

[2] C. J. Morley, "Surfactant treatment for premature babies—a review of clinical trials," Archives of Disease in Childhood, **66**, 445 (1991)

[3] H. A. Stone, A. Ajdari, "Hydrodynamics of particles embedded in a flat surfactant layer overlying a subphase of finite depth," J. Fluid. Mech. **369,** 151 (1998)

[4] T. M. Fischer, "The drag on needles moving in a Langmuir Monolayer," J. Fluid. Mech **498**, 123 (2004)

[5] P. G. Saffman and M. Delbrück, "Brownian motion in biological membranes," Proc. Natl. Acad. Sci. USA **72**, 3111 (1975)

[6] V. Prasad, S. A. Koehler, and E. R. Weeks, "Two-particle microrheology of quasi-2D viscous systems," Phys. Rev. Lett. **97**, 176001 (2006)

[7] P. Dhar, Y. Cao, T. M. Fischer, J. A. Zasadzinski, "Active interfacial shear microrheology of aging protein films," Phys. Rev. Lett. **104**, 016001 (2010)

[8] J. Ding, H. E. Warriner, J. A. Zasadzinski, "Viscosity of two-dimensional suspensions," Phys. Rev. Lett. **88**, 168102 (2002)

[9] C. Alonso, A. Waring, J. A. Zasadzinski, "Keeping lung surfactant where it belongs: protein regulation of two-dimensional viscosity," Biophysical Journal, **89**, 266 (2005)

[10] J. Ding, H. E. Warriner, J. A. Zasadzinski, D. K. Schwartz, "Magnetic needle viscometer for Langmuir monolayers," Langmuir, *18*, 2800-2806 (2002)

[11] D. J. Griffiths, *Introduction to Electrodynamics*, (Prentice Hall, New Jersey, 1999) 3rd ed, Chap. 5, 202

[12] G. Fuller, K. –S Yim, C. Brooks, D. Olson, C. Frank, "The rheology of two-dimensional systems" Korea-Australia Rheol. J. *11*, 321-328. (1999)

[13] S. Reynaert, C. F. Brooks, P. Moldenaers, J. Vermant, G. G. Fuller, "Analysis of the magnetic rod interfacial stress rheometer," J. Rheol., *52*(1), 261-285 (2008)

[14] M. H. Lee, C. P.Lapointe, D. H. Reich, K. J. Stebe, R. L. Leheny, "Interfacial Hydrodynamic Drag on Nanowires Embedded in Thin Oil Films and Protein Layers," Langmuir, *25*(14), 7976-7982 (1999)

[15] P. Chen, S. Lahooti, Z. Policova, M. A. Cabrerizo-Vilchez, A. W. Neumann, "Concentration dependence of the film pressure of human serum albumin at the water/decane interface," Colloids and Surfaces B: Biointerfaces, **6**, 279 (1996)

[16] J. C. Crocker, D. G. Grier, "Methods of Digital Video Microscopy for Colloidal Studies," Journal of Colloid and Interface Science, **179**, No. 1, 298 (1996)

[17] A. Anguelouch, R. L. Leheny, D. H. Reich, "Application of ferromagnetic nanowires to interfacial microrheology," Appl. Phys. Lett. **89**, 111914 (2006)